

## Gas-phase IR spectra of intact $\alpha$ -helical coiled coil protein complexes

Kevin Pagel<sup>a,\*</sup>, Peter Kupser<sup>b</sup>, Frauke Bierau<sup>b</sup>, Nicolas C. Polfer<sup>c,1</sup>, Jeffrey D. Steill<sup>c</sup>,  
Jos Oomens<sup>c</sup>, Gerard Meijer<sup>b</sup>, Beate Kokscha<sup>a</sup>, Gert von Helden<sup>b</sup>

<sup>a</sup> Institut für Chemie und Biochemie, Freie Universität Berlin, Takustr. 3, 14195 Berlin, Germany

<sup>b</sup> Fritz-Haber-Institut der Max-Planck-Gesellschaft, Faradayweg 4-6, 14195 Berlin, Germany

<sup>c</sup> FOM Institute for Plasmaphysics, Edisonbaan 14, 3439 MN Nieuwegein, The Netherlands

### ARTICLE INFO

#### Article history:

Received 19 January 2009

Received in revised form 25 February 2009

Accepted 25 February 2009

Available online 14 March 2009

Dedicated to Professor M.T. Bowers on the occasion of his 70's birthday.

#### Keywords:

Secondary structure

Protein complex

Infrared multiphoton dissociation

Electrospray ionization

$\alpha$ -Helix

### ABSTRACT

Electrospray ionization (ESI) is the softest ionization method that is currently available and it is widely accepted, that ESI generated ions of proteins and protein assemblies at certain conditions retain characteristic aspects of their solution-state conformation. ESI mass spectrometry (MS) therefore evolved as a useful tool to obtain information on composition, stoichiometry, and dynamics of non-covalently associated protein complexes. While tertiary structure information of proteins can be obtained from ion mobility spectrometry (IMS), only a few techniques yield direct information on the secondary structure of gas-phase peptides and proteins. We present here the mid-IR spectroscopic secondary structural analysis of three de novo designed  $\alpha$ -helical coiled coil model peptides and their non-covalently associated complexes in the gas-phase. The conformational stability of such coiled coil peptides in solution is primarily driven by aggregation. Isolated monomers usually remain unfolded. Two of the investigated peptides were designed to assemble into stable  $\alpha$ -helical complexes in acidic solution, while the third one remains monomeric and unfolded at these conditions. Monomer ions of all three peptides show comparable photodissociation IR spectra and therefore suggest an unfolded conformation in the gas phase. In contrast, considerable C=O stretch (amide-I) and N-H bend (amide-II) band shifts have been observed for the dimers which is consistent with an elevated H-bond content. These findings provide evidence that at least a fraction of the condensed phase  $\alpha$ -helical structure is retained in the gas-phase coiled coil complexes.

© 2009 Elsevier B.V. All rights reserved.

### 1. Introduction

In recent years, electrospray ionization (ESI) mass spectrometry (MS) evolved as a valuable tool to enable the analysis and characterization of the stoichiometry, dynamics, and shape of non-covalently associated protein complexes [1–6]. Instrument modifications that involve changes in the differential pumping region [7] as well as the development of nano-ESI sources [8] have been pioneering achievements, which nowadays make mass spectrometry a key-technique in structural genomics and proteomics [6]. Very recent investigations showed that even membrane protein complexes, which are usually extremely difficult to analyze, can be transferred intact into a mass spectrometer [9].

A crucial requirement for the analysis of an intact protein complex in the gas phase is the (at least partial) conservation of the

condensed-phase conformation. Several investigations on large protein assemblies provided evidence that important structural features such as a compact globular shape, secondary structure elements, hydrogen bonding patterns, and characteristic quaternary contacts can be maintained at certain instrument and solution conditions [10]. Soft landing approaches for example showed that viruses retain their shape and infectivity after ES ionization, transfer, and deposition on a surface placed at the end of the mass spectrometer [11]. In addition, ion mobility spectrometry (IMS) [12], especially when coupled to MS, can provide valuable insights on the gas-phase conformation of proteins and protein complexes [13,14]. Investigations on the undecameric complex of the tryptophan-RNA binding attenuation protein (TRAP) for example revealed, that the characteristic ring-like topology present in solution can be retained in the absence of solvent [15]. Furthermore, IMS was successfully applied to characterize the quaternary organization of small, soluble A $\beta$ 42 oligomers, which are thought to be the toxic component in Alzheimer's disease [16].

On the other end of the molecular scale, there have been various combined IMS and molecular dynamics (MD) studies on small peptides and peptide complexes, which adopt unique and defined in vacuo conformations [17,18]. Most of these peptides are

\* Corresponding author. Current address: University of Cambridge, Department of Chemistry, Lensfield Road, Cambridge, CB2 1EW, UK. Tel.: +44 1223 763844.

E-mail address: [kp345@cam.ac.uk](mailto:kp345@cam.ac.uk) (K. Pagel).

<sup>1</sup> Current address: Department of Chemistry, University of Florida, Gainesville, FL 32611, USA.

alanine- and/or glycine-rich which makes them easy to calculate and understand, but also hardly soluble in aqueous solutions. As a consequence, often rather harsh source conditions and a high acetic acid or trifluoroacetic acid (TFA) content are required to electrospray these peptides. However, various well defined conformations such as isolated  $\alpha$ -helices [19,20], helix-turn-helix motifs [18], and non-covalently associated helices [21] with partially impressive thermal stability have been observed for these systems. According to the properties of the gas-phase environment, mainly charge–charge, charge–dipole, and dipole–dipole interactions have been found to contribute to their conformational stability.

Despite the enormous differences between small in vacuo peptides and large solution-like protein assemblies, there is a common problem – a tremendous lack of knowledge on the secondary structure level. In the condensed phase, direct measurements of the secondary structure can be easily performed using circular dichroism [22] or infrared (IR) spectroscopy [23]. Until a few years ago, there was no similar method for gas-phase structural analyses, but recently IR spectroscopy became available to gain secondary structure information of biomolecular ions in the gas phase. A limited amount of species has been investigated since then, including amino acids [24], dipeptides [25,26], tripeptides [27], longer polypeptides [28–30,32,33], and the full length protein cytochrome C [34]. However, to date relatively little has been done on the gas-phase IR spectroscopic analysis of protein complexes. More importantly, nothing is known on the secondary structural differences between protein complexes and their corresponding subunits in the gas phase. This kind of information is of outstanding importance, because a quaternary organization is often crucial for folding (and also misfolding) in solution.

Within this paper we present the gas-phase IR spectroscopic analysis of one of the smallest and most stable protein assemblies known from nature – the  $\alpha$ -helical coiled coil. The structural characterization in solution was performed by CD spectroscopy, while infrared multiphoton dissociation (IRMPD) spectroscopy was employed to obtain secondary structure data of dimeric coiled coil complexes and their corresponding monomers. Perceptible differences between both species suggest that the cooperative, oligomerization-driven folding known for coiled coils in solution to some extent also exists in the solvent-free environment. In addition, our data provide evidence that at least a fraction of the helical conformation is retained in the gas phase.

## 2. Experimental

### 2.1. Peptide synthesis and purification

Model peptides VW01, VW02, and VW03 were synthesized by standard Fmoc chemistry on Fmoc-Leu-OWang resin (0.68/0.71 mmol/g) using a 431 A peptide synthesizer (Applied Biosystems, Darmstadt, Germany). The peptides were cleaved from the resin by reaction with 3 mL of a solution containing 5% (v/v) triisopropylsilane, 0.1% (v/v) water, and 94.9% (v/v) TFA. Purification was carried out by preparative reversed-phase high-performance liquid chromatography (HPLC) on a Vydac C4 column. The molecular weight of the products was determined by MALDI-TOF mass spectrometry using a Voyager MALDI-TOF Mass spectrometer (PerSeptive/Applied Biosystems, Darmstadt, Germany) and its purity was determined by analytical HPLC on a Merck LaChrom system (Merck, Darmstadt, Germany) equipped with a Vydac C4 (10  $\mu$ m) column (Grace Vydac, Columbia, MD, USA). The gradient used was similar to those of the preparative HPLC.

VW02Abz was synthesized by a solid phase assembly using a Multi-Syntech Syro XP peptide synthesizer (MultisynTech, Witten, Germany) by Fmoc strategy on Fmoc-Leu-OWang resin (0.65 mmol/g). In contrast to VW02, VW02Abz was N-terminally

capped with anthranilic acid (Abz).<sup>2</sup> The peptide was cleaved from the resin by reaction with 4 mL of a solution containing 10% (w/v) triisopropylsilane, 1% (w/v) water, and 89% (w/v) TFA. The crude product was purified by reversed-phase HPLC on a Knauer smart-line manager 5000 system (Knauer, Berlin, Germany) equipped with a C8 (10  $\mu$ m) LUNA™ Phenomenex column (Phenomenex, Torrance, CA, USA). The peptide was eluted with a linear gradient of acetonitrile/water/0.1% trifluoroacetic acid and identified by MS using an Agilent 6210 ESI-ToF LC/MS spectrometer (Agilent Technologies, Santa Clara, CA, USA) with direct infusion via a Harvard Apparatus 11plus syringe pump (Harvard Apparatus, Holliston, MA, USA). Purity was determined by analytical HPLC on a Merck LaChrom system (Merck, Darmstadt, Germany) equipped with a C8 (10  $\mu$ m) LUNA™ Phenomenex column (Phenomenex, Torrance, CA, USA). The gradient used was similar to those of the preparative HPLC.

### 2.2. CD spectroscopy

CD measurements of peptides in buffer were carried out on a J-715 spectrometer equipped with a temperature controller (Jasco, Easton, MD, USA) using a quartz cell of mm path length. Spectra were recorded at 25 °C from 200 to 240 nm at 0.5–0.2 nm resolution with a scan rate of 20 nm/min and a sensitivity of 100 mdeg. Three scans were acquired and averaged for each sample. Raw data were manipulated by smoothing and subtraction of buffer spectra. The concentration was 0.8 mg/mL, which corresponds to approximately 250  $\mu$ M. CD values are given in mdeg and were not converted into molar ellipticities, since concentration in solution was not determined independently and only roughly estimated by the weighted amount of peptide. The following buffers were used: pH 4.0, pH 5.0: 10 mM acetate buffer; pH 7.4, 8.0: 10 mM Tris–HCl buffer.

### 2.3. Infrared photodissociation experiments

The experiments were performed at the free electron laser facility FELIX [35] (Nieuwegein, the Netherlands) by using the Fourier-transform ion cyclotron (FT-ICR) mass spectrometer [36]. Ions were generated via electrospray ionization. In order to avoid higher-order aggregation, which might affect the ESI process, exclusively freshly prepared samples were used for the presented experiments. Therefore, 0.15 mg of peptide was dissolved freshly in 1 mL NH<sub>4</sub>OFor buffer (10 mM, pH 4.5, Fisher Scientific, Schwerte, Germany). Subsequently, the pH was adjusted to 4.5 using diluted formic acid solution and 40% MeOH (v/v, Acros Organics, Geel, Belgium) was added to obtain a stable and reproducible spray. The solution was sprayed via a syringe pump Harvard Apparatus 11plus (Harvard Apparatus, Holliston, MA, USA) and a standard Z-spray source (Waters Corporation, Milford, MA, USA) connected to the mass spectrometer. The ESI generated ions were transported and accumulated in a hexapole ion trap and subsequently transferred into a home-built FT-ICR mass spectrometer that is optically accessible via a KRS-5 window at the back end. After trapping and mass-selective isolation of the charged molecules of interest inside the ICR cell, the ions were irradiated by IR photons of the free electron laser FELIX. When the IR light is resonant with an IR active vibrational mode in the molecule, this results in the absorbance of many photons, which causes dissociation of the ion (IRMPD).

Monitoring the fragmentation yield or the depletion of the parent ion signal as a function of IR wavelength leads to the IR spectra.

<sup>2</sup> 2-Aminobenzoic acid (Abz, common name anthranilic acid) is often used as UV-label to enable a photometric concentration determination in solution. Unpublished results from our group indicate that this modification has no noticeable influence on the condensed phase folding properties of a 26-residue coiled coil peptide.

Recent studies showed that the so-obtained spectra are not entirely identical to linear IR absorption spectra, but can be very close to it [37]. The output of FELIX is continuously tunable over a range of 40–2000  $\text{cm}^{-1}$ . In the presented experiment only the range from 1300 to 1850  $\text{cm}^{-1}$  was scanned. The light consists of macropulses of about 5  $\mu\text{s}$  length at a repetition rate of 10 Hz, which contain 0.3–5 ps long micropulses with a micropulse spacing of 1 ns. In the present experiment, macropulse energies were in the range 35 mJ with a bandwidth of approximately 1%.

### 3. Results and discussion

#### 3.1. Peptide design

Within this study, three different  $\alpha$ -helical coiled coil model peptides have been investigated. Coiled coils, also often referred to as leucine zipper proteins, are very common in nature and approximately 3–5% of all amino acids in naturally occurring peptides and proteins are involved in their formation [38]. Therefore, coiled coils have been studied extensively within the last 20 years, which led to a profound understanding of the interactions that govern thermodynamic stability and specificity of folding; making it one of the best understood protein folding motifs [38,39]. Today, artificial coiled coils with properties that are optimized for a particular purpose or application can be designed de novo according to well established principles [40–42].

$\alpha$ -Helical coiled coils typically consist of two to five right-handed  $\alpha$ -helices which are wound around one another forming a left-handed supercoil. Fig. 1a and b exemplarily shows the molecular modeling structure of an antiparallel 41-residue coiled coil. The primary structure of each helix is characterized by a periodicity of seven residues, the so-called 4-3 heptad repeat which is commonly denoted  $(\text{abcdefg})_n$ . For design purposes, these seven residues are often presented in a so-called helical wheel diagram, which, in a simplified manner, depicts the alignment of residues along the helical axis (Fig. 1c). Positions a and d are typically occupied by apolar residues (Leu, Ile, Val, Met) that form a special interaction surface at the interface of the helices by hydrophobic core packing (“knobs-into-holes”) [38–40]. In contrast, positions e and g are frequently occupied by charged amino acids (most commonly Glu, Arg, and Lys) that form inter-helical Coulomb interactions [39]. Polar residues are often found in the remaining heptad repeat positions b, c, and f, which are solvent exposed at the opposite side of the helical cylinder.

In solution, the hydrophobic core provides the major contribution to the thermodynamic stability of the  $\alpha$ -helical coiled coil. In contrast, the inter-helical ionic pairing positions e and g mainly dictate the specificity of folding (parallel versus antiparallel) and promote the preference for homo- or heterotypic  $\alpha$ -helical coiled coil formation [43–45]. An additional interaction domain, which is not related to the coiled coil oligomerization, is formed by intramolecular Coulomb interactions between positions c/g and b/e, respectively. These interactions indirectly influence the stability of  $\alpha$ -helical coiled coil complexes by stabilizing or destabilizing the single helices [46,47]. The combination of all three previously described interactions makes coiled coil folding a highly cooperative process, i.e., the helical structure cannot exist without oligomerization and vice versa. As a result, isolated monomers as they for example occur at very low concentrations remain unfolded in solution.

Idealized coiled coils are often extraordinarily resistant to urea- and temperature-driven denaturation in solution. However, conditions in the gas phase are explicitly different, which may affect the previously described coiled coil recognition motifs tremendously. Due to the absence of bulk water hydrophobic interactions are thought to be reduced to their van der Waals fraction, while

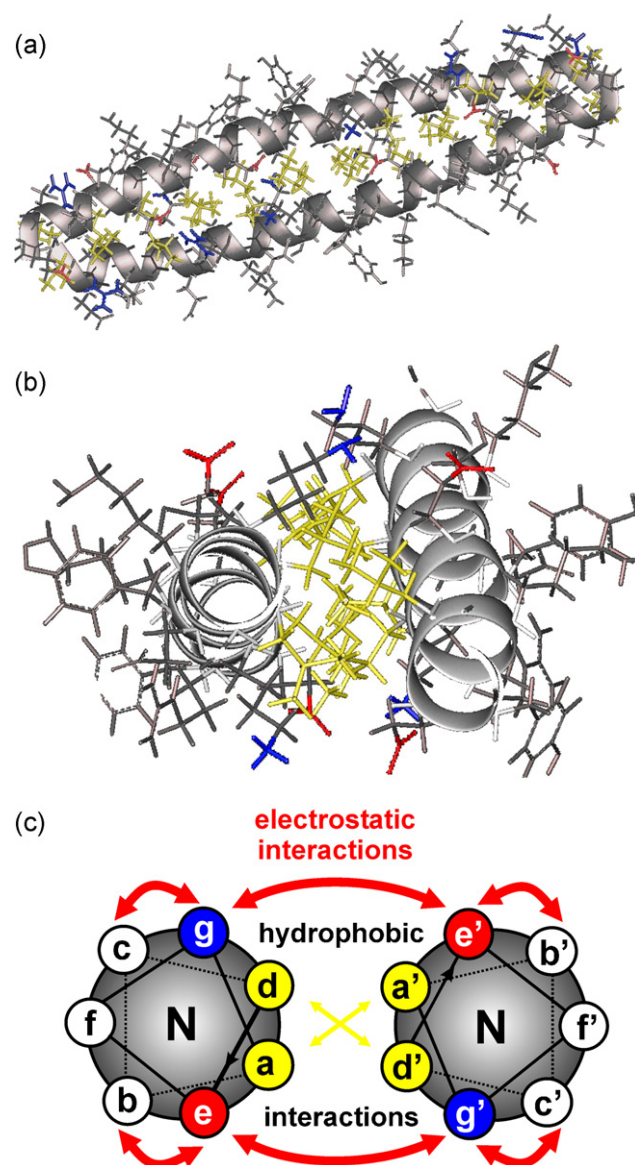


**Fig. 1.** Molecular modeling structure representing the solution-state conformation of a dimeric coiled coil peptide. (a) View perpendicular to the axis of the helix and (b) view along the helical axis. (c) Helical wheel diagram of a parallel coiled coil showing the three recognition motifs. Yellow residues represent hydrophobic interactions, while coulomb interactions are occurring between negatively (red) and positively charged residues (blue). (For interpretation of the references to color in this figure caption, the reader is referred to the web version of the article.)

Coulomb interactions and hydrogen bonds are assumed to increase substantially in the gas phase [10,48]. Even though hydrophobic core packing is the major determinant for coiled coil folding in solution, ESI generated ions of oligomers can be transferred, stored and detected in the solvent-free environment of a mass spectrometer [45,49,50]. Surprisingly, this is even possible at conditions and instrument setups which are not particularly suitable for the analysis of intact protein complexes. From these findings, the question arises how oligomers of coiled coil peptides are held together in the gas phase and, more importantly, whether this is accompanied by a conservation of the helical conformation. If so, perceptible differences in the gas-phase IR spectra of monomers and oligomers should occur. To shed light on these questions, three different 26-residue coiled coil model peptides have been designed, characterized and investigated by gas-phase mid-IR photodissociation spectroscopy.



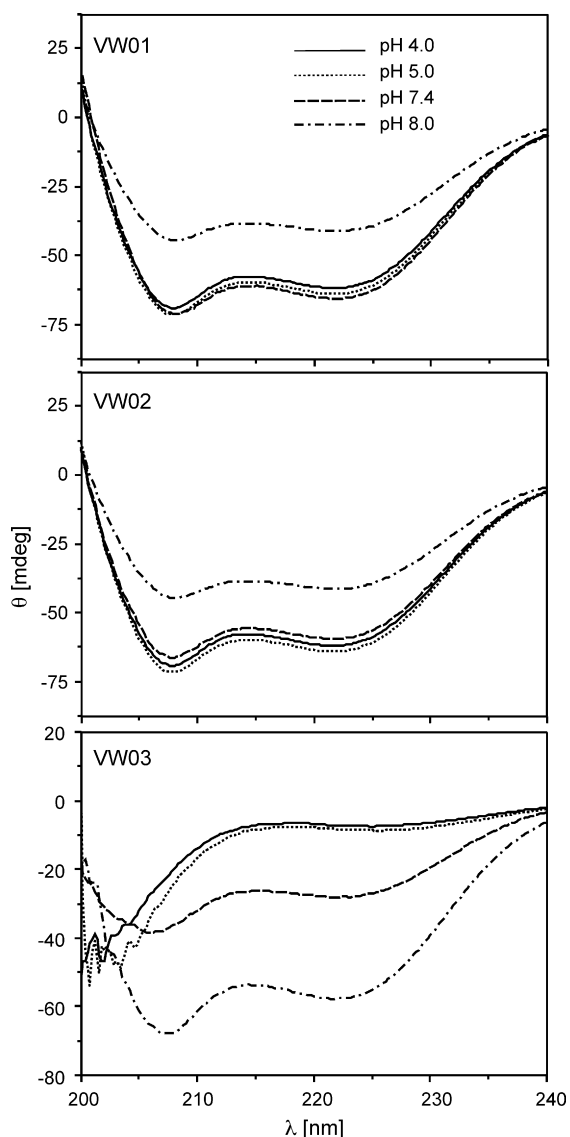


**Fig. 3.** CD spectra of approximately 250  $\mu\text{M}$  peptide VW01, VW02, and VW03 at pH 4.0, 5.0, 7.4, and 8.0. VW01 and VW02 exhibit a clear helical conformation at all investigated pH values while VW03 remains unfolded at pH 4.0 and 5.0.

observed at concentrations as low as 20  $\mu\text{M}$ , however no higher oligomers were found.

### 3.4. Photodissociation spectra of monomers

In order to record IR spectra, all ions, except the  $m/z$  ions of interest, are ejected by employing SWIFT excitation. The remaining ions are then irradiated by FELIX, and the fragmentation yield is recorded as a function of IR wavelength. Because of the limited mass resolution, it cannot be fully excluded that the observed monomer ions are slightly superimposed by the corresponding even-charged dimers. However, due to the much greater relative intensities of monomers in comparison to dimers it can be assumed that the majority of ions is indeed in the monomer state.

Fig. 5 shows the acquired IRMPD spectra for VW01, VW02Abz, and VW03 monomer units for several charge states. Fragmentation occurs into several product ions, which were not assigned. In all spectra, two main peaks can be recognized. The peaks at higher wavenumbers fall into the C=O stretching (amide-I) vibration region while the peaks at lower wavenumbers are in a region, where N–H bending (amide-II) modes are expected to occur. In the

top part, the spectra for VW01 having the charge states +3, +4, and +5 are shown. The peaks in the amide-I region are all centered near  $1662\text{ cm}^{-1}$  and their width seems to increase slightly with increasing charge state. At the blue side of this band, a shoulder near  $1745\text{ cm}^{-1}$  is observed, which is more pronounced in the spectrum of the +5 ion of VW01 than in the spectra of the other two peptides. In the amide-II region of the VW01 spectra, the peaks for the +3 and +4 species are virtually identical. For the +5 ion, however, the amide-II peak becomes more intense, while also shifting to lower frequency and broadening.

The spectra of VW02Abz in the charge states +3, +4, and +5 are shown in the center of Fig. 5. Similar peak positions, widths and trends as in the spectra of VW01 are observed. The main differences to the case of VW01 is that for VW02Abz in the +3 charge state, the peak near  $1745\text{ cm}^{-1}$  is missing and that in the spectra of the +4 ion, the amide-I and -II bands are broader and slightly shifted.

For the VW03 monomer, only the +4 and +5 charge states could be generated at ion densities sufficient to record IR spectra. These are shown in the lower part of Fig. 5. The spectra of those ions are similar to the spectra of the lower charge states of VW01 and VW02Abz.

For all three VW monomers considered, the spectra appear very similar. One exception are the spectra of VW01 and VW02Abz in the +5 charge states, for which the amide-II bands are red shifted, as well as displaying increased intensities. Further, for all ions, with increasing charge state, the amide-I bands shows a slight broadening towards the lower-frequency side. Nonetheless, the average position of the amide-I band is the same for all three ions for their respective charge states. This suggests that all the monomer ions have similar structures.

### 3.5. Photodissociation spectra of dimers

For VW01 and VW02Abz, the dimer ions having a +5 charge are observed in quantities sufficient to allow for the recording of IR spectra. For VW03, no gas-phase dimers could be observed at the used experimental condition. When the  $[(\text{VW01})_2 + 5\text{H}]^{5+}$  or  $[(\text{VW02Abz})_2 + 5\text{H}]^{5+}$  are isolated and irradiated by FELIX at wavelengths that allow for photon absorption and subsequent fragmentation, the corresponding +3 and +2 monomer ions are observed as fragmentation products (Fig. 4b). In Fig. 6, the IRMPD spectra of  $[(\text{VW01})_2 + 5\text{H}]^{5+}$  and  $[(\text{VW02Abz})_2 + 5\text{H}]^{5+}$  are shown. For comparison, the corresponding spectra of the +3 monomer ions (which are also shown in Fig. 5) are shown with dashed lines. The spectra of  $[(\text{VW01})_2 + 5\text{H}]^{5+}$  and  $[(\text{VW02Abz})_2 + 5\text{H}]^{5+}$  show amide-I and -II resonances that occur at virtually the same position and have the same width. This suggests that the structures of both types of dimers are very similar. In both dimer spectra, the amide-I and -II resonances are broader and shifted, compared to those of the monomers. For the amide-I mode this shift is about  $11\text{ cm}^{-1}$  to the red, while for the amide-II band, a  $23\text{ cm}^{-1}$  shift to the blue is observed. Different to the behavior of the monomers, some background fragmentation of the dimers can be observed at wavelengths that do not correspond to intense bands, such as the amide-I and -II resonances, thus resulting in an elevated baseline in their spectra.

### 3.6. Structural implications for monomers and dimers

Based on the IR spectra, all monomer ions appear to have similar structures. For VW03, intramolecular electrostatic interactions strongly destabilize the helical conformation and the solution data at comparable pH values as used in the gas-phase experiments reveal non-helical (presumably monomer) structures. It is thus likely that in the gas phase, the structure present for VW03 is non-helical and more disordered, random-coil like. For VW01

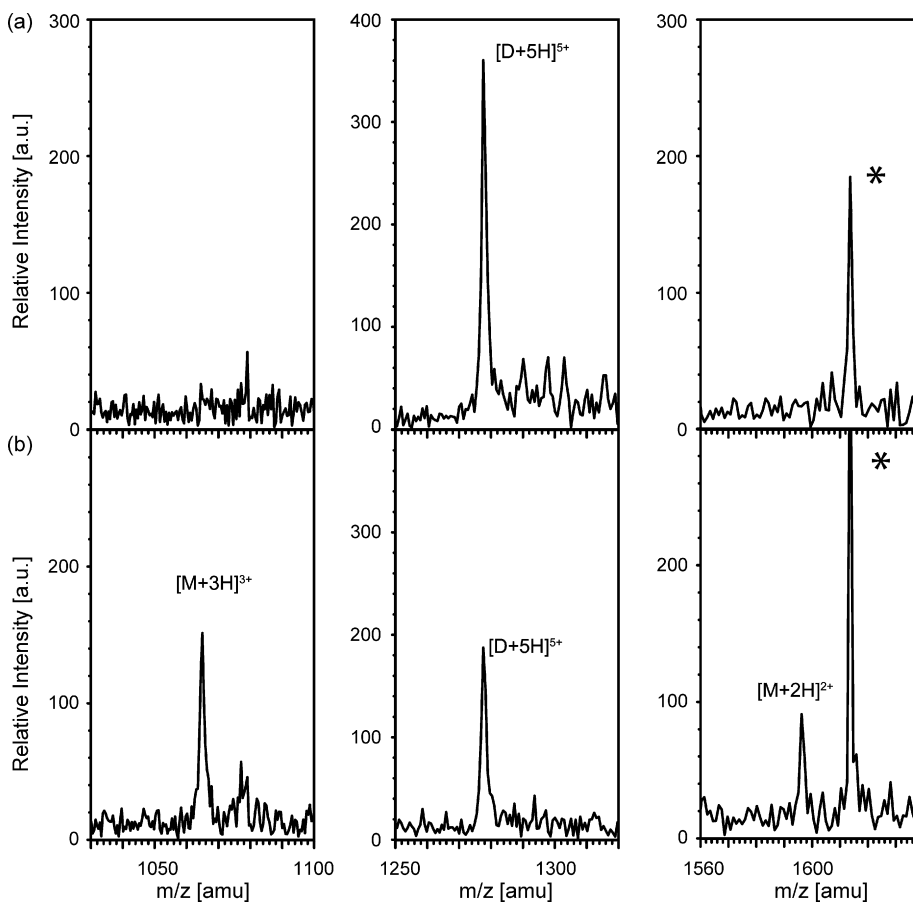


**Fig. 4.** Mass spectra of swift-isolated VW01 dimers (center,  $[D+5H]^{5+}$ ) after irradiation with FELIX at (a) 5.5  $\mu\text{m}$  and (b) 6.1  $\mu\text{m}$ . IRMPD at 6.1  $\mu\text{M}$  results in a fragmentation of the complex into the corresponding monomers (left,  $[M+3H]^{3+}$ ; right  $[M+2H]^{2+}$ ) while no dissociation occurs at 5.5  $\mu\text{M}$ . Asterisks indicate electromagnetic interferences which occur sample-independently.

and VW02Abz, intramolecular electrostatic interactions may support helix formation even for monomers, however, the similarity of their spectra to those of VW03 points to disordered random-coil structures for these peptides as well. With increasing charge state, the shoulder near  $1750\text{ cm}^{-1}$  is observed to become more prominent. A resonance at that position reveals the presence of non-hydrogen bonded C=O groups, either on the peptidic backbone, on the C-terminus or on a Glu side chain [53]. Likely additional protonation sites of the VW molecules are either the previously neutral basic sidechains or the deprotonated  $\text{COO}^-$  groups. Which of these processes occurs depends on the internal charge balance of the molecule. VW01 has seven basic Lysine residues, seven acidic glutamic acid residues as well as an acidic and a basic terminus. The amino acid content of VW02Abz is similar, except the N-terminus, which is capped with anthranilic acid. This cap also possesses a basic- $\text{NH}_2$  group, however, its pK of 4.9 is significantly lower than that of a free N-terminus. In solution, at pH levels such as employed here, nearly all carboxylic acid groups of VW01 should be deprotonated and all amino groups protonated, resulting in an overall uncharged, or slightly positively charged molecule. For VW02Abz, the amino group at the anthranilic acid will be only partially protonated. When such an internal charge distribution persists in the gas phase, excess protons will be added to the  $\text{COO}^-$  groups. This is in line with the observation that the intensity of the  $1750\text{ cm}^{-1}$  mode increases with the charge state. The situation is different in case of VW03. Here, four additional arginine residues are present. It is thus likely that additional protons (up to a charge state of +7) will be added to the lysine or arginine side chains. In agreement with that, no  $1750\text{ cm}^{-1}$  mode is present in the spectra.

In the dimer spectra, the amide-I mode is shifted to the red and the amide-II mode to the blue, compared to the monomer spectra. The similarity between the two dimer spectra and the dissimilarity to the monomer spectra suggests that both dimers have comparable structures that are distinctively different from those of the monomers. However, a clear structural assignment on basis of the absolute band positions is difficult. To date, only a very limited amount of peptides and proteins with defined secondary structure have been characterized by gas-phase IR spectroscopy. Unlike in solution there are no reference values that clearly reveal a certain conformation. Nevertheless, the general tendencies known from the condensed phase [54] are also valid in the gas phase. Considering this, the observed shifts in the amide-I and -II positions are consistent with an increase in hydrogen bonding. Hydrogen bonds lead to a removal in electron density from the carbonyl oxygens, which in turn reduces the C=O stretch frequency (i.e., red shift of the amide-I band). Conversely, amide-II band are blueshifted as a result of hydrogen bonding interactions. This can be rationalized by the fact that a hydrogen bond introduces "stiffness" into the N-H bending mode, thus requiring more energy for this motion. In solution, especially the amide-I mode strongly depends on the underlying secondary structure and red-shifts up to  $50\text{ cm}^{-1}$  are observed for H-bond-rich  $\beta$ -sheet proteins and protein aggregates [54]. The correlation between secondary structure and position of the amide-II band is less straightforward in comparison to the amide-I band [54]. Nevertheless, perceptible band shifts are also observed for this frequency region in solution. In the presented gas-phase spectra, perceptible band shifts in both amide modes are evident. According to the previously mentioned condensed

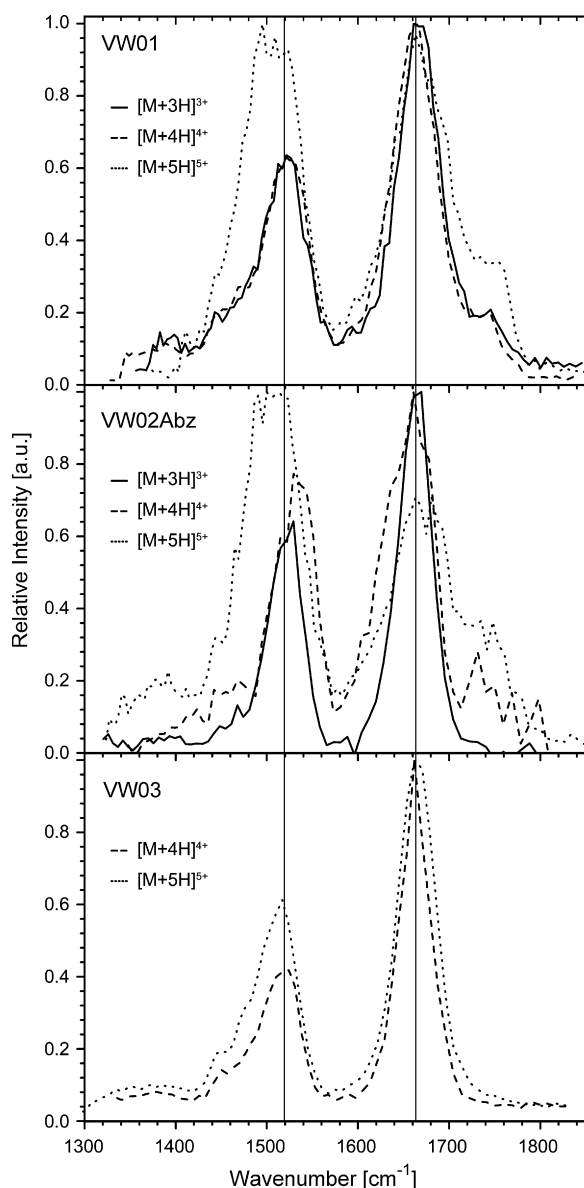


**Fig. 5.** Mid-IR photodissociation spectra of VW01, VW02ABz, and VW03 monomers at charge state +3, +4, +5. For VW03 charge state +3 was not observed.

phase principles, this provides evidence for an elevated hydrogen bond content in the dimer ions. Band broadening in case of the dimer ions furthermore supports this hypothesis [55]. Therefore, it is likely that at least a fraction of the helical conformation is retained in the gas phase. Unlike in solution, the band shift is more pronounced for the amide-II band. It remains elusive if this is a unique behavior of the investigated peptides or a general difference between condensed phase and gas-phase IR spectroscopy of proteins.

In the condensed phase, intramolecular as well as inter-helical interactions strongly support the coiled coil structure. Those interactions include electrostatic (salt-bridge) interactions, hydrogen bonding as well as hydrophobic interactions between the central leucine residues. In the condensed phase, charged parts of the molecule will be tightly solvated by polar solvents. This solvation causes an effective steric and electrostatic shielding and reduces the relative importance of the electrostatic interactions. In the gas phase, no solvent shielding is present and the electrostatics will become the most important type of interaction. For VW01 and VW02Abz, such interactions will still stabilize a coiled coil confor-

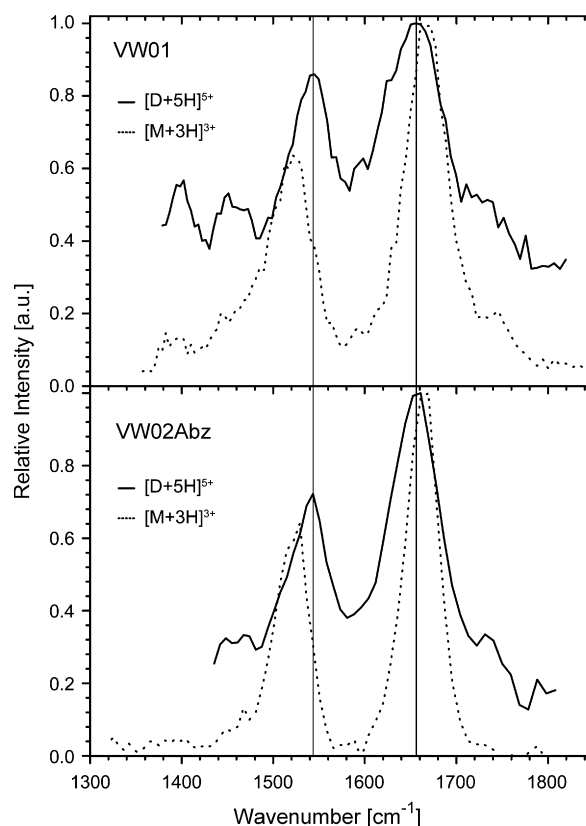


**Fig. 6.** Mid-IR photodissociation spectra of VW01 and VW02Abz dimers at charge state +5. The corresponding +3 monomers are shown for comparison purposes.

mation, but as those interactions become much more important compared to the hydrophobic interactions, it is not clear if the hydrophobic core will be conserved in the gas phase. Indeed, this is what is observed in preliminary MD simulations, where the leucine residues are found on the outside of a coiled coil structure.<sup>3</sup> In conclusion, it is likely that the spectra we observe in Fig. 6 result from helix-rich coiled coil-like assemblies in the gas phase, however structural differences to the condensed phase situation are also expected.

#### 4. Conclusion

We present here the IR spectroscopic characterization of three de novo designed  $\alpha$ -helical coiled coil peptides and their dimeric complexes in the gas phase. As shown by CD spectroscopy, two of these peptides assemble into non-covalent  $\alpha$ -helical coiled coil complexes at acidic pH, while the third peptide remains fully unfolded and monomeric at these conditions. Comparable mid-IR photodissociation spectra have been obtained for monomer ions of all three peptides, which points to a similar random-coil-like conformation in the gas phase. Non-covalently associated dimer ions have been observed for peptides one and two, which, in comparison to monomers, exhibit considerably different photodissociation IR spectra. The position of the amide-I (C=O stretch) mode is shifted 11  $\text{cm}^{-1}$  to the red, while the amide-II band (N-H bend) is shifted 23  $\text{cm}^{-1}$  to the blue. This suggests an increased H-bond content in the dimers, which provides evidence that at least a certain fraction of the condensed phase helical structure is also retained in the gas-phase coiled coil dimer ions.

<sup>3</sup> Unpublished results.

## Acknowledgements

This work has been supported by the European Community – Research Infrastructure Action under the FP6 “Structuring the European Research Area” Programme (through the Integrated Infrastructure Initiative “Integrating Activity on Synchrotron and Free Electron Laser Science.”). We gratefully acknowledge the support by the ‘Stichting voor Fundamenteel Onderzoek der Materie’ (FOM) for providing the required beam time on FELIX. We furthermore thank Dr. B. Redlich, Dr. A.F.G. van der Meer, and the FELIX staff for their competent assistance during the experiments. Dipl. Biochem. Toni Vagt is gratefully acknowledged for help in peptide synthesis and CD spectroscopy. Last, but not least we like to thank Dr. Carsten Baldauf for molecular dynamics simulations, which were unfortunately too preliminary to be included in this paper.

## References

- [1] J.A. Loo, *Mass Spectrom. Rev.* 16 (1997) 1.
- [2] R.H.H. van den Heuvel, A.J.R. Heck, *Curr. Opin. Chem. Biol.* 8 (2004) 519.
- [3] A.J.R. Heck, R.H.H. van den Heuvel, *Mass Spectrom. Rev.* 23 (2004) 368.
- [4] A.E. Ashcroft, *Nat. Prod. Rep.* 22 (2005) 452.
- [5] J.L.P. Benesch, C.V. Robinson, *Curr. Opin. Struct. Biol.* 16 (2006) 245.
- [6] J.L.P. Benesch, B.T. Ruotolo, D.A. Simmons, C.V. Robinson, *Chem. Rev.* 107 (2007) 3544.
- [7] F. Sobott, H. Hernandez, M.G. McCammon, M.A. Tito, C.V. Robinson, *Anal. Chem.* 74 (2002) 1402.
- [8] M.S. Wilm, M. Mann, *Int. J. Mass Spectrom. Ion Process.* 136 (1994) 167.
- [9] N.P. Barrera, N. Di Bartolo, P.J. Booth, C.V. Robinson, *Science* 321 (2008) 243.
- [10] B.T. Ruotolo, C.V. Robinson, *Curr. Opin. Chem. Biol.* 10 (2006) 402.
- [11] G. Siuzdak, B. Bothner, M. Yeager, C. Brugidou, C.M. Fauquet, K. Hoey, C.-M. Change, *Chem. Biol.* 3 (1996) 45.
- [12] G. von Helden, T. Wyttenbach, M.T. Bowers, *Science* 267 (1995) 1483.
- [13] B.T. Ruotolo, J.L.P. Benesch, A.M. Sandercock, S.-J. Hyung, C.V. Robinson, *Nat. Protoc.* 3 (2008) 1139.
- [14] T. Wyttenbach, M.T. Bowers, *Ann. Rev. Phys. Chem.* 58 (2007) 511.
- [15] B.T. Ruotolo, K. Giles, I. Campuzano, A.M. Sandercock, R.H. Bateman, C.V. Robinson, *Science* 310 (2005) 1658.
- [16] S.L. Bernstein, T. Wyttenbach, A. Baumketner, J.-E. Shea, G. Bitan, D.B. Teplow, M.T. Bowers, *J. Am. Chem. Soc.* 127 (2005) 2075.
- [17] M.F. Jarrold, *Phys. Chem. Chem. Phys.* 9 (2007) 1659 (and literature cited therein).
- [18] A.E. Counterman, D.E. Clemmer, *J. Am. Chem. Soc.* 123 (2001) 1490.
- [19] R.R. Hudgins, M.A. Ratner, M.F. Jarrold, *J. Am. Chem. Soc.* 120 (1998) 12974.
- [20] R.R. Hudgins, M.F. Jarrold, *J. Phys. Chem. B* 104 (2000) 2154.
- [21] R. Sudha, M. Kohtani, M.F. Jarrold, *J. Phys. Chem. B* 109 (2005) 6442.
- [22] G.D. Fasman, *Circular Dichroism and the Conformational Analysis of Biomolecules*, Plenum Press, New York, 1996.
- [23] W.K. Surewicz, H.H. Mantsch, D. Chapman, *Biochemistry* 32 (1993) 389.
- [24] M.F. Bush, J. Oomens, R.J. Saykally, E.R. Williams, *J. Phys. Chem. A* 112 (2008) 8578.
- [25] B. Lucas, G. Grégoire, J. Lemaire, P. Maître, J.-M. Ortega, A. Rupenyán, B. Reimann, J.P. Schermann, C. Desfrancois, *Phys. Chem. Chem. Phys.* 6 (2004) 2659.
- [26] N.C. Polfer, J. Oomens, R.C. Dunbar, *Chem. Phys. Chem.* 9 (2008) 579.
- [27] R. Wu, T.B. McMahon, *J. Am. Chem. Soc.* 129 (2007) 11312.
- [28] N.C. Polfer, J. Oomens, *Phys. Chem. Chem. Phys.* 9 (2007) 3804.
- [29] N.C. Polfer, J. Oomens, S. Suhai, B. Paizs, *J. Am. Chem. Soc.* 129 (2007) 5887.
- [30] T.D. Vaden, S.A.N. Gowers, T.S.J.A. de Boer, J.D. Steill, J. Oomens, L.C. Snoek, *J. Am. Chem. Soc.* 130 (2008) 14640.
- [31] J.A. Stearns, O.V. Boyarkin, T.R. Rizzo, *J. Am. Chem. Soc.* 129 (2007) 13820.
- [32] J.A. Stearns, C. Seabiy, O.V. Boyarkin, T.R. Rizzo, *Phys. Chem. Chem. Phys.* 11 (2009) 125.
- [33] J. Oomens, N. Polfer, D.T. Moore, L. van der Meer, A.G. Marshall, J.R. Eyler, G. Meijer, G. von Helden, *Phys. Chem. Chem. Phys.* 7 (2005) 1345.
- [34] D. Oepts, A.F.G. van der Meer, P.W. van Amersfoort, *Infrared Phys. Technol.* 36 (1995) 297.
- [35] J.J. Valle, J.R. Eyler, J. Oomens, D.T. Moore, A.F.G. van der Meer, G. von Helden, G. Meijer, C.L. Hendrickson, A.G. Marshall, G.T. Blakney, *Rev. Sci. Instrum.* 76 (2005) 023103.
- [36] J. Oomens, B.G. Sartakov, G. Meijer, G. von Helden, *Int. J. Mass Spectrom.* 254 (2006) 1.
- [37] J.M. Mason, K.M. Arndt, *ChemBioChem* 5 (2004) 170.
- [38] Y.B. Yu, *Adv. Drug Deliv. Rev.* 54 (2002) 1113.
- [39] D.N. Woolfson, *Adv. Protein Chem.* 70 (2005) 79.
- [40] K. Pagel, T. Vagt, T. Kohajda, B. Kokschi, *Org. Biomol. Chem.* 3 (2005) 2500.
- [41] K. Pagel, B. Kokschi, *Curr. Opin. Chem. Biol.* 12 (2008) 730.
- [42] M.G. Oakley, J.J. Hollenbeck, *Curr. Opin. Struct. Biol.* 11 (2001) 450.
- [43] D.G. Gurnon, J.A. Whitaker, M.G. Oakley, *J. Am. Chem. Soc.* 125 (2003) 7518.
- [44] K. Pagel, K. Seeger, B. Seiwert, A. Villa, A.E. Mark, S. Berger, B. Kokschi, *Org. Biomol. Chem.* 3 (2005) 1189.
- [45] P. Burkhard, S. Ivaninskii, A. Lustig, *J. Mol. Biol.* 318 (2002) 901.
- [46] M. Hoshino, N. Yumoto, S. Yoshikawa, Y. Goto, *Protein Sci.* 6 (1997) 1396.
- [47] A. Patriksson, E. Marklund, D. van der Spoel, *Biochemistry* 46 (2007) 933.
- [48] H. Wendt, E. Durr, R.M. Thomas, M. Przybylski, H.R. Bosshard, *Protein Sci.* 4 (1995) 1563.
- [49] S. Witte, F. Neumann, U. Krawinkel, M. Przybylski, *J. Biol. Chem.* 271 (1996) 18171.
- [50] K. Pagel, S.C. Wagner, K. Samedov, H. von Berlepsch, C. Böttcher, B. Kokschi, *J. Am. Chem. Soc.* 128 (2006) 2196.
- [51] K. Pagel, S.C. Wagner, R. Rezaei Araghi, H. von Berlepsch, C. Böttcher, B. Kokschi, *Chem. Eur. J.* 14 (2008) 11442.
- [52] J.M. Bakker, C. Plützer, I. Hünig, T. Häber, I. Compagnon, G. von Helden, G. Meijer, K. Kleinermanns, *ChemPhysChem* 6 (2005) 120.
- [53] A. Barth, C. Zscherp, *Q. Rev. Biophys.* 35 (2002) 369.
- [54] D.T. Moore, J. Oomens, L. van der Meer, G. von Helden, G. Meijer, J. Valle, A.G. Marshall, J.R. Eyler, *ChemPhysChem* 5 (2004) 740.